INFECTIOUS DISEASE

Productive Replication of Ebola Virus Is Regulated by the c-Abl1 Tyrosine Kinase

Mayra García,[1] Arik Cooper,[1] Wei Shi,[1] William Bornmann,[2] Ricardo Carrion,[3] Daniel Kalman,[4] Gary J. Nabel[1]*

Ebola virus causes a fulminant infection in humans resulting in diffuse bleeding, vascular instability, hypotensive shock, and often death. Because of its high mortality and ease of transmission from human to human, Ebola virus remains a biological threat for which effective preventive and therapeutic interventions are needed. An understanding of the mechanisms of Ebola virus pathogenesis is critical for developing antiviral therapeutics. Here, we report that productive replication of Ebola virus is modulated by the c-Abl1 tyrosine kinase. Release of Ebola virus–like particles (VLPs) in a cell culture cotransfection system was inhibited by c-Abl1–specific small interfering RNA (siRNA) or by Abl-specific kinase inhibitors and required tyrosine phosphorylation of the Ebola matrix protein VP40. Expression of c-Abl1 stimulated an increase in phosphorylation of tyrosine 13 (Y^{13}) of VP40, and mutation of Y^{13} to alanine decreased the release of Ebola VLPs. Productive replication of the highly pathogenic Ebola virus Zaire strain was inhibited by c-Abl1–specific siRNAs or by the Abl-family inhibitor nilotinib by up to four orders of magnitude. These data indicate that c-Abl1 regulates budding or release of filoviruses through a mechanism involving phosphorylation of VP40. This step of the virus life cycle therefore may represent a target for antiviral therapy.

INTRODUCTION

Viruses of the Filoviridae family (Ebola and Marburg) are highly lethal pathogens that cause fever, diffuse bleeding, and hypotensive shock in humans and nonhuman primates. These negative-strand RNA viruses are composed of a genome about 19 kb in size. Among the seven gene products of Ebola virus, nucleoprotein (NP), VP35, and VP24 are necessary and sufficient for nucleocapsid assembly (*1*), and additional expression of VP40 permits release of filamentous virus-like particles (VLPs) (*2*, *3*). Many viruses exploit cellular components to complete their life cycle (*4*). Accordingly, c-Abl1 and related tyrosine kinases (TKs) have been implicated in actin motility and affect replication of certain DNA viruses and bacteria (*5*–*9*); however, it was unknown whether such kinases could affect negative-strand and highly pathogenic RNA viruses through similar mechanisms. We hypothesized that c-Abl1 may modulate the trafficking or release of Ebola virus through effects on viral or cellular gene products. To test this possibility, we examined the effect of c-Abl1 on Ebola virus assembly and release using a transfection system that results in formation and release of VLPs (*1*, *3*) and during acute infection in vitro. We report that c-Abl1 regulates both Ebola VLP formation and viral replication through a mechanism involving posttranslational modification of the Ebola *VP40* gene product.

RESULTS

Egress of Ebola VLPs is inhibited by c-Abl small interfering RNAs

Transfection of expression vectors encoding VP24, VP35, VP40, NP, and glycoprotein (GP) into the 293 human renal epithelial cell line induced VLPs (*1*–*3*) detectable by both immunoprecipitation and electron microscopy (fig. S1). To determine whether c-Abl1 affected VLP release, we knocked down c-Abl1 or the related c-Abl2 with specific small interfering RNAs (siRNAs) (Fig. 1A, lanes 1 to 6). c-Abl2 siRNA had no effect on c-Abl1 levels (Fig. 1A, lane 1 versus lane 3) or vice versa (Fig. 1A, lane 4 versus lane 5). Notably, transfection of c-Abl1 siRNA decreased the quantity of VLPs by ~5-fold or by ~2.5-fold as measured by NP or VP40 protein levels, respectively, after immunoprecipitation with GP (Fig. 1A, lane 11). No effect was observed on intracellular levels of Ebola virus NP or VP40 proteins (Fig. 1A, lanes 7 to 9). The effect was specific; similar effects were evident with three individual siRNAs for c-Abl1 (Fig. 1B, lanes 14 to 16 and 22 to 24), whereas c-Abl2 siRNA or a control siRNA had no detectable effect (Fig. 1A, lanes 10 and 12), and c-Abl1 siRNAs did not alter expression of an unrelated control protein, eIF4E (eukaryotic initiation factor 4E) (Fig. 1B, compare lane 13 with lanes 14 to 16). Moreover, c-Abl1 siRNAs had no effect on intracellular levels of Ebola virus NP or VP40 proteins (Fig. 1B, lanes 17 to 20). c-Abl1 siRNAs also decreased VLP release (Fig. 1B, lanes 21 to 24) as measured by NP and VP40 protein levels, suggesting that Abl1 regulates egress of preassembled VLPs from the cell.

Release of Ebola VLPs is decreased by c-Abl1 TK inhibitors

We next determined the effect of specific Abl-family TK inhibitors on VLP production. Imatinib and nilotinib inhibit c-Abl1 kinase activity and are used clinically for treatment of chronic myelogenous leukemia, a disease caused by translocations or mutations that dysregulate c-Abl1 (*10*–*15*). Incubation of 293T cells with imatinib (Fig. 1C, left panel) or nilotinib (Fig. 1C, right panel) 12 to 18 hours after transfection of Ebola virus plasmids resulted in a dose-dependent reduction in VLP release measured by NP and VP40 protein levels. No toxicity was observed at the selected concentrations (Fig. 2A). Neither drug reduced the formation of intracellular nucleocapsids, as detected by transmission electron microscopy (Fig. 2B) or Western analysis (Fig. 2C), or affected intracellular levels of NP, VP40, and VP35 (Fig. 1C, upper panels, and Fig. 2C, lanes 1 and 2), suggesting a specific effect of

[1]Vaccine Research Center, National Institute of Allergy and Infectious Diseases, National Institutes of Health, Bethesda, MD 20892, USA. [2]Organic Chemistry Section, M. D. Anderson Cancer Center, University of Texas, Houston, TX 77030, USA. [3]Department of Virology and Immunology, Texas Biomedical Research Institute, San Antonio, TX 78227, USA. [4]Department of Pathology and Laboratory Medicine, Emory University, Atlanta, GA 30322, USA.
*To whom correspondence should be addressed. E-mail: gnabel@nih.gov

the drugs on VLP trafficking or egress. By contrast, treatment with drugs was without effect on levels of GP (fig. S2, A and B), a protein reported to enhance release of VLPs (*16*).

In addition to nucleocapsid-containing VLPs, we assessed the effects of inhibiting c-Abl1 on VP40-induced VLPs lacking nucleocapsid. c-Abl1–specific siRNAs reduced release of VP40 VLPs by the same degree as observed for complete VLPs (Fig. 3, A and B). Moreover, release of VP40 VLPs was likewise reduced by nilotinib (Fig. 3C).

c-Abl1 TK phosphorylates Ebola virus proteins

To define potential viral targets of c-Abl1, we assessed phosphorylation of tyrosine residues within Ebola virus proteins. Notably, VP40 contains a sequence surrounding Y^{18} that is homologous to a sequence in the Tir protein of enteropathogenic *Escherichia coli*, which serves as an Abl/Tec phosphorylation site and an SH2-binding site (*17*). To determine whether VP40 can serve as an Abl TK substrate, we transfected 293T cells with a c-Abl1 expression vector in conjunction with an Ebola virus VP40 plasmid. Transfected c-Abl1 was catalytically active as evidenced by autophosphorylation on Y^{412} (fig. S3A, lanes 2 and 5), an effect inhibited by imatinib (fig. S3A, lane 3) and nilotinib (fig. S3A, lane 6). Upon immunoprecipitation, VP40 was both tyrosine-phosphorylated and associated with c-Abl1 (Fig. 4A, lane 6, upper and middle panels). The effect appeared specific; both phosphorylation of VP40 and its association with c-Abl were antagonized by nilotinib (Fig. 4A, lane

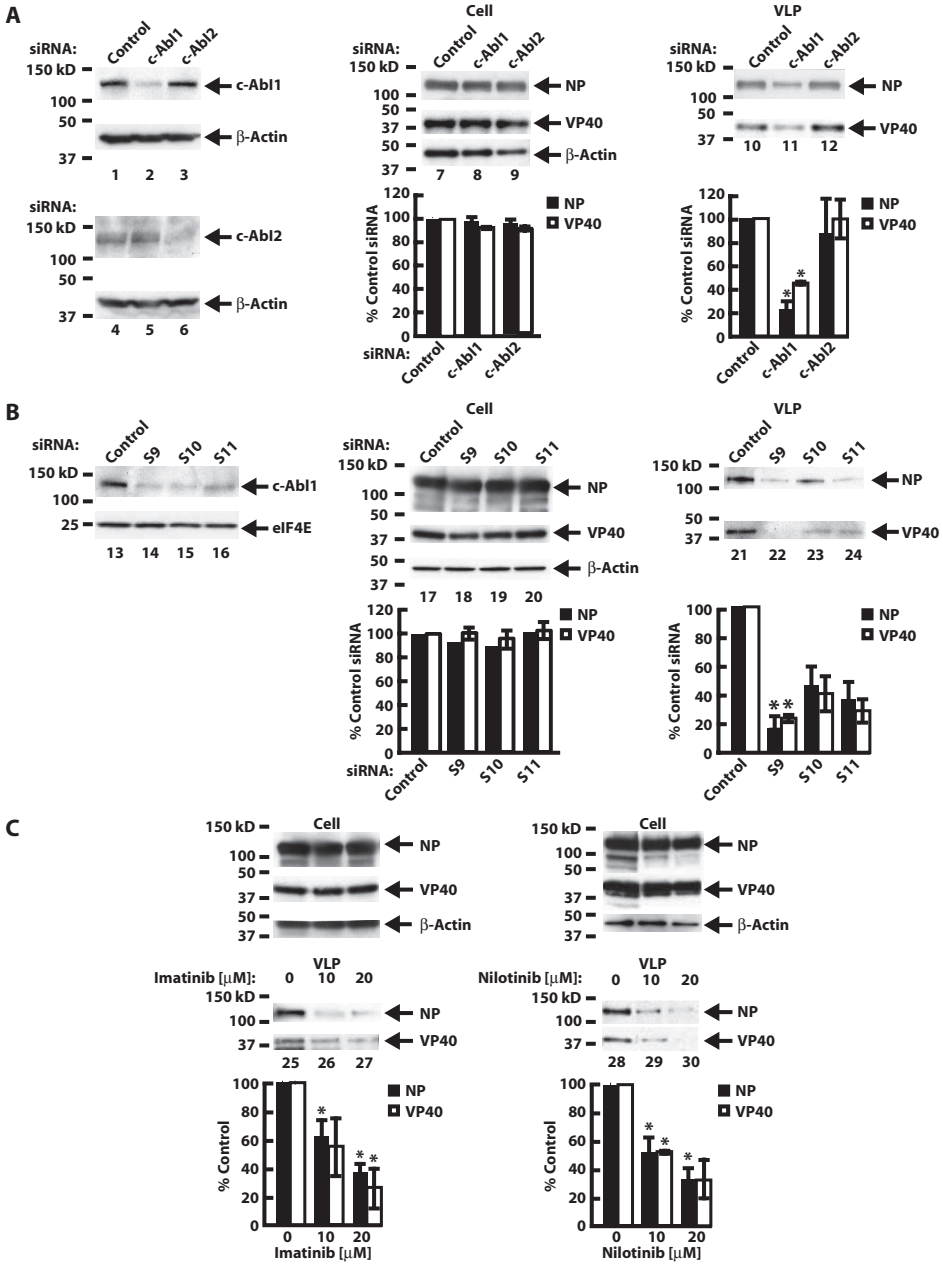

Fig. 1. Effect of c-Abl1 knockdown and kinase inhibition on Ebola VLP release in transfected 293T cells. (**A**) Knockdown of c-Abl1 (lanes 1 to 3) or c-Abl2 (lanes 4 to 6) using nontargeting siRNA control or siRNA targeting c-Abl1 or c-Abl2 confirmed by Western analysis in cell lysates with antibodies specific to either c-Abl1 (lanes 1 to 3) or c-Abl2 (lanes 4 to 6). β-Actin was used as a loading control. The results are representative of five independent experiments. 293T cells were transfected with plasmids encoding VP24, VP35, VP40, NP, and GP. In all cases, Ebola VLPs were analyzed by immunoprecipitation with GP followed by Western blotting for NP and VP40 (lanes 10 to 12). Cell lysates are shown in lanes 7 to 9. Data represent means ± SEM of individual measures with cells from four independent experiments. Significant differences by paired Student's *t* test between test and control siRNAs are indicated. **P* < 0.05. (**B**) Knockdown of c-Abl1 using a nontargeted siRNA control (lane 13) or three individual siRNAs (S9, S10, and S11) targeting c-Abl1 (lanes 14 to 16) was analyzed by Western analysis in cell lysates, with eIF4E as a loading control. NP and VP40 present in cell lysates were determined (lanes 17 to 20), and Ebola VLPs in supernatants were measured as in (A) after knockdown with c-Abl1 individual siRNAs (lanes 21 to 24). Data represent means ± SEM of individual measures with cells from three independent experiments. Significant differences by paired Student's *t* test between test and control siRNAs are indicated. **P* < 0.05. For (A) and (B), quantitation of NP and VP40 protein bands is expressed as a percentage of the intensity of the siRNA control band (lower panels). (**C**) Western analysis of Ebola VLP release for NP and VP40 content with imatinib (lanes 25 to 27) or nilotinib (lanes 28 to 30). Water was used as control for imatinib and DMSO for nilotinib. Quantitation of NP and VP40 was performed relative to the intensity of the solution control band. Data are presented as means ± SEM of individual measures with cells from eight (for NP) and three (for VP40) independent experiments. Significant differences by paired Student's *t* test between drug and vehicle control are indicated. **P* < 0.05.

6 versus lane 8). Moreover, kinase-dead c-Abl1 did not induce detectable phosphorylation of VP40 or association with c-Abl upon immunoprecipitation (fig. S3B, lane 11 versus lane 12). Finally, cotransfection of c-Abl1 siRNAs with the VP40 and c-Abl1 expression vectors inhibited tyrosine phosphorylation of VP40 and association with c-Abl1 (Fig. 4B, lane 12 versus lane 14), an effect similar to that observed with nilotinib (Fig. 4B, lane 12 versus lane 13). Activation of c-Abl by overexpression, or its inhibition by drug treatment, resulted in increased VP40 expression with a fold change of 1.75 ± 0.19, a statistically significant difference (P = 0.02). Although the basis for such changes are unclear, this effect could result from either increased transcription or reduced turnover of VP40. However, these changes are independent of the effects on VLPs, a phenomenon that is observed only when c-Abl1 kinase activity is inhibited.

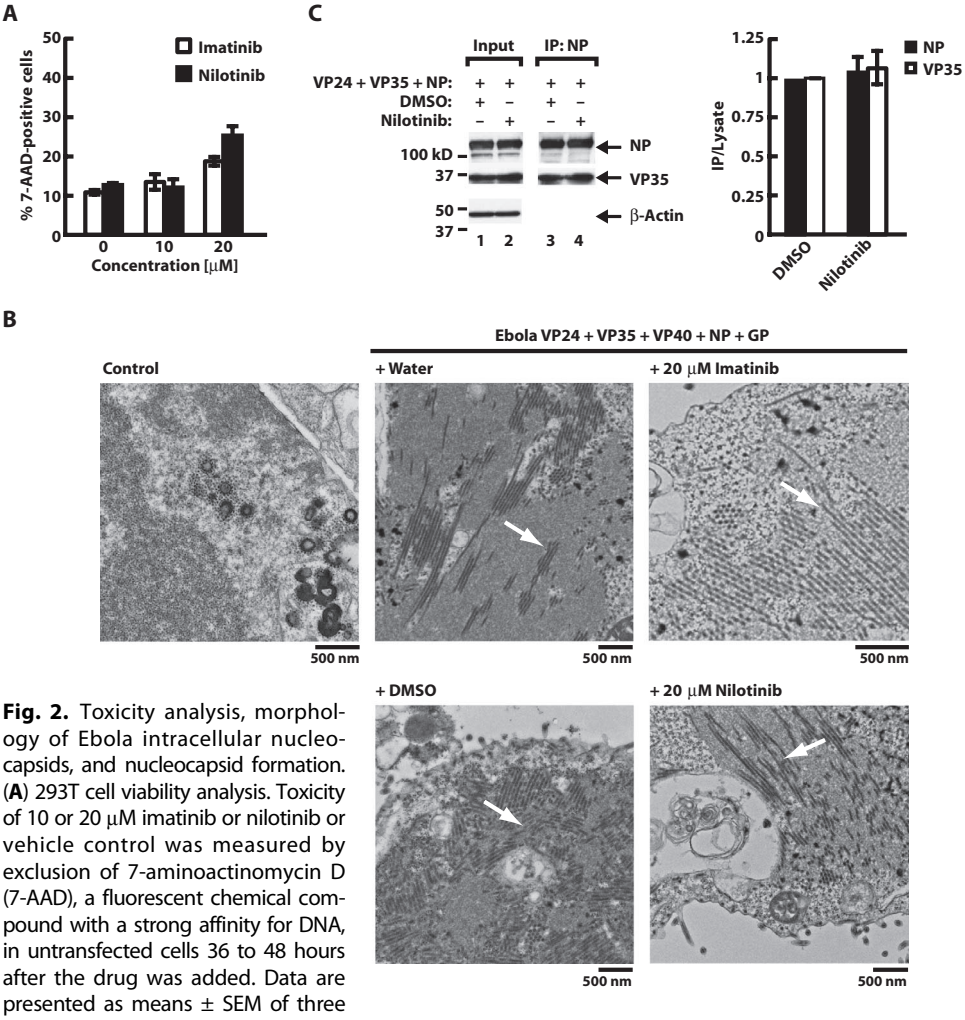

Fig. 2. Toxicity analysis, morphology of Ebola intracellular nucleocapsids, and nucleocapsid formation. (**A**) 293T cell viability analysis. Toxicity of 10 or 20 μM imatinib or nilotinib or vehicle control was measured by exclusion of 7-aminoactinomycin D (7-AAD), a fluorescent chemical compound with a strong affinity for DNA, in untransfected cells 36 to 48 hours after the drug was added. Data are presented as means ± SEM of three independent experiments. (**B**) Morphology of Ebola virus nucleocapsids in 293T cells transfected with empty vector (left panel) or the five Ebola virus plasmids in combination with water or DMSO controls (middle panels) or 20 μM drug treatments (right panels) seen intracellularly (white arrows) by electron microscopy. Size standards are shown. (**C**) Nucleocapsid formation. Effect of nilotinib (lane 4) in nucleocapsid formation on cells transfected with VP24, VP35, and NP. Anti-NP antibody was used for immunoprecipitation (IP) of nucleocapsids. Quantitation of NP and VP35 was performed relative to the intensity of the DMSO control band (lane 3). Input amount of protein is shown in lanes 1 and 2. Data are presented as means ± SEM of individual measures with cells from three independent experiments.

Endogenous c-Abl1 also phosphorylates VLP-associated VP40

Without cotransfection, immunoprecipitation with a phosphotyrosine monoclonal antibody (mAb) or c-Abl1 mAb followed by Western analysis with anti-VP40 confirmed that tyrosine phosphorylation of VP40 (Fig. 4C, lane 19 versus lane 20) and its association with endogenous c-Abl1 (Fig. 4C, lane 22 versus lane 23) were likewise sensitive to nilotinib. Phosphorylation of VP40 by endogenous c-Abl1 was confirmed after c-Abl1 siRNA treatment followed by immunoprecipitation with a phosphotyrosine mAb and Western analysis with anti-VP40 (Fig. 4D, lane 27 versus lane 28). Using available antibodies, we could not resolve endogenous phospho–c-Abl upon immunoprecipitation, either because the levels were too low or because the protein cycles into a dephosphorylated state. Incorporation of phosphorylated VP40 into VLPs was observed by Western analysis of isolated VLPs through a sucrose cushion (Fig. 4E, lane 35). Finally, the association of VP40 with NP (*2*, *16*, *18*) was reduced by nilotinib (Fig. 4F, lane 44 versus lane 45) to background levels (Fig. 4F, lane 42), indicating a reduced NP-VP40 interaction. Together, these data provide evidence that c-Abl1 associates with VP40 and mediates its phosphorylation and that phosphorylated VP40 is incorporated into VLPs.

VP40 is phosphorylated by c-Abl1 on Y^{13}

To assess the role of VP40 phosphorylation in Ebola virus VLP release, we determined the sites of tyrosine phosphorylation in VP40 by mass spectrometry (MS) after cotransfection of VP40 and c-Abl1. Tryptic peptides containing phosphorylated tyrosine residues were predicted to increase the mass/charge ratio (m/z) ratio by 40 compared to unphosphorylated peptides, and matrix-assisted laser desorption ionization (MALDI) analysis detected several peptides with such m/z deviations, including tyrosine 13 (Y^{13}) (Fig. 5A, right versus left panel) and Y^{292} (fig. S4A, right versus left panel). A similar modification of VP40 Y^{13} was evident in the absence of cotransfected c-Abl1 (fig. S4B, right versus left panel).

We then asked whether c-Abl1 mediated phosphorylation of a mutated VP40 containing a substitution of alanine for tyrosine at position 13 ($VP40^{Y13A}$). No phosphorylation of immunoprecipitated $VP40^{Y13A}$ was detectable by Western analysis (Fig. 5B, lane 6 versus lane 8) even upon cotransfection with c-Abl1. In contrast, $VP40^{Y292A}$ remained phosphorylated (fig. S4C, lane 10 versus lane 14), whereas the double mutant (fig. S4C, lane 10 versus lane 16) did not, suggesting that Y^{13}, but not Y^{292}, was a target of c-Abl1.

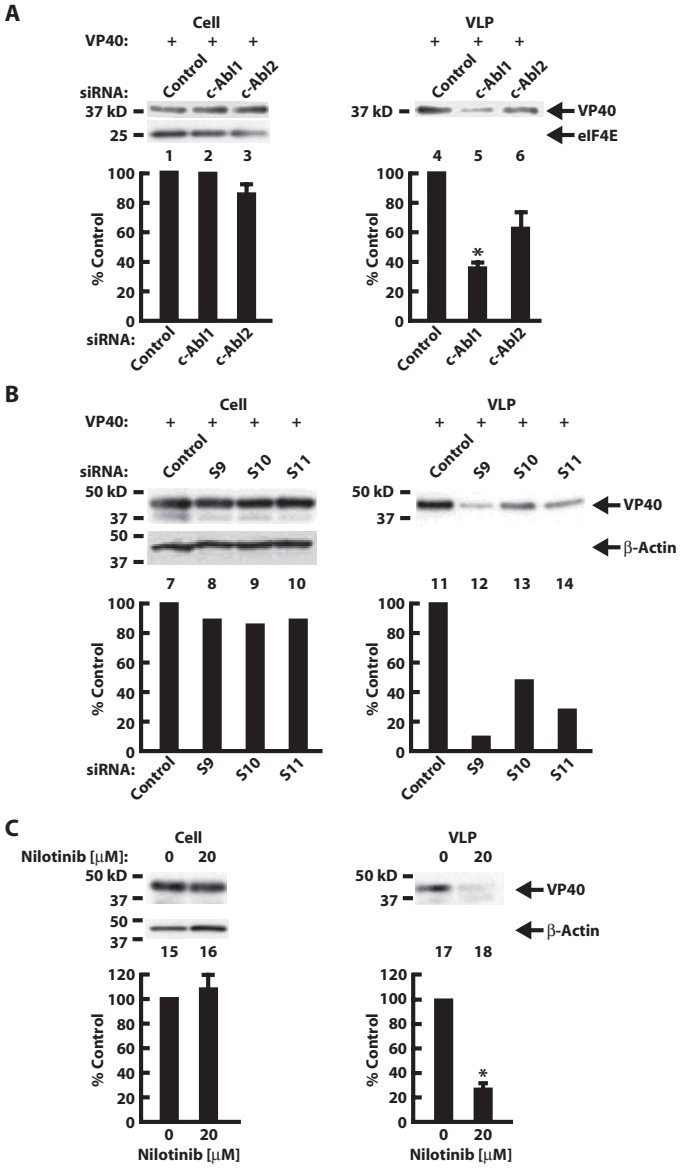

Fig. 3. c-Abl1–specific siRNA and nilotinib effects on VP40 VLP egress. 293T cells were transfected with plasmid encoding VP40. (**A** and **B**) VP40 VLPs were analyzed by immunoprecipitation with mAb anti-FLAG followed by Western analysis for VP40 after transfection with a pool (A) (lanes 4 to 6) or individual (B) (lanes 11 to 14) siRNAs specific to c-Abl1. Cell lysates are shown in lanes 1 to 3 and 7 to 10. VP40 levels in VLPs were normalized to inputs. Quantitation of VP40 protein bands is expressed as a percentage of the intensity of the siRNA control band. Data represent means ± SEM of individual measures with cells from three independent experiments for (A). Significant differences by paired Student's *t* test between test and control siRNAs are indicated. **P* < 0.05. (**C**) Western analysis of VP40 VLP release after immunoprecipitation with mAb anti-FLAG (lanes 17 and 18). Cells were incubated with 20 μM nilotinib (lanes 16 and 18). DMSO was used as the solution control (lanes 15 and 17). Cell lysates are shown in lanes 15 and 16. Quantitation of VP40 was performed relative to the intensity of the solution control band. Data are presented as means ± SEM of individual measures with cells from three independent experiments. Significant differences by paired Student's *t* test between drug and vehicle control are indicated. **P* < 0.05.

Phosphorylation of Y^{13} by c-Abl is required for Ebola VLP egress

To determine whether phosphorylation of Y^{13} was involved in Ebola VLP egress, we cotransfected wild-type VP40 or the $VP40^{Y13A}$ mutant with the other Ebola virus plasmids and assessed VLP release. No difference in intracellular VP40 or NP levels was evident (Fig. 5C, left panel, lane 10 versus lane 11). However, with the Y13A mutant, levels of released VLP-associated NP were reduced by 84% (Fig. 5, C, lane 13 versus lane 14, and D). Cotransfection of VP40 and Nedd4, a protein known to interact at position Y^{13} of the matrix protein (*19*), did not affect the interaction with Nedd4 in the presence of nilotinib (fig. S5A, bar graph) yet disrupted interactions with c-Abl1 (Fig. 4A, lane 6 versus lane 8). In addition, Y13A disrupted the Nedd4 interaction with VP40 (fig. S5B, left graph), whereas the interaction with c-Abl was retained (fig. S5B, right graph). Collectively, these data suggest that phosphorylation of VP40 on Y^{13} by c-Abl1 is necessary for the egress of VLPs, an effect that appears independent of Nedd4.

c-Abl1 TK inhibitors reduce productive replication of wild-type Ebola virus

We next determined whether c-Abl1 regulates productive replication of Zaire Ebola virus, a strain that is lethal in humans and nonhuman primates identified after an outbreak in 1976 in the Ebola River valley of Zaire, now the Democratic Republic of the Congo (*20*, *21*). Treatment of Vero E6 cells with the S9 or S10 c-Abl1 siRNAs reduced Zaire Ebola virus production by 8- to 10-fold 7 days after infection (Fig. 6A), measured by relative levels that generated 50% of a tissue culture infectious dose ($TCID_{50}$). After incubation of Vero cells with nilotinib, Ebola virus infectious virion production decreased by up to about four logs 8 days after infection (Fig. 6B). Notably, there was no detectable cytopathic effect of the drug alone (fig. S6, A and B), and nilotinib had no effect on infection by an unrelated virus, adenovirus 5 (fig. S6C), confirming the specificity of this inhibition. To discriminate an effect of the drug on entry versus egress, we used a luciferase-pseudotyped HIV virus with Ebola virus envelope to infect 293A cells. Ebola virus GP–mediated entry was not affected by nilotinib at concentrations up to 20 μM, the highest tested (fig. S6D). The greater fold reduction evident with nilotinib (Fig. 6B) compared to c-Abl1 siRNA treatment (Fig. 6A) was likely due to the greater penetration of the drug in all cells compared with the lower transfection efficiency of siRNA (fig. S6E). Collectively, these data demonstrate that c-Abl1 regulates Ebola Zaire growth in vitro and that c-Abl1 antagonists inhibit productive Ebola virus replication.

DISCUSSION

The process of filovirus assembly and release is not well understood, in part due to the difficulty of generating viral recombinants and the challenges of working with the virus under high level biocontainment. Nevertheless, information on these mechanisms is critical to the development of preventive and antiviral therapies. Assembly of Ebola virus requires the generation and transport of the viral genome–protein complex to the site of budding where the infectious virus is released from cells (*2*). The assembly of the viral nucleocapsid complex requires expression of three viral genes: *NP*, *VP35*, and *VP24* (*1*). The matrix protein VP40 is required both for the transport of nucleocapsids to the

cell surface through interactions with microtubules (*2*, *4*) and for the incorporation of nucleocapsids into virions (*2*, *3*).

VP40 also plays an important role in the morphogenesis of the filamentous virions and subsequent budding (*19*, *20*, *22*–*24*). In mammalian cells, expression of VP40 alone produces membranous projections with a filamentous morphology similar to Ebola virus (*3*, *25*, *26*), although these particles do not contain other viral proteins or NP and thus do not represent authentic VLPs. NP has also been shown to enhance VP40 budding activity, suggesting an interaction between the proteins (*16*, *18*). The limitations of working with the virus in biosafety level 4 (BSL4) make it technically impossible to characterize the mechanism of egress with infectious virus. Therefore, we have chosen to carry out mechanistic studies using in vitro models that recapitulate relevant aspects of Ebola infection under BSL2 conditions and permit extensive experimental manipulation. Here, we demonstrate that Abl1 TK regulates formation of VLPs and stimulates productive replication of Ebola virus in cells using specific siRNAs and pharmacological inhibitors. Even though there is a c-Abl1$^{-/-}$ cell line

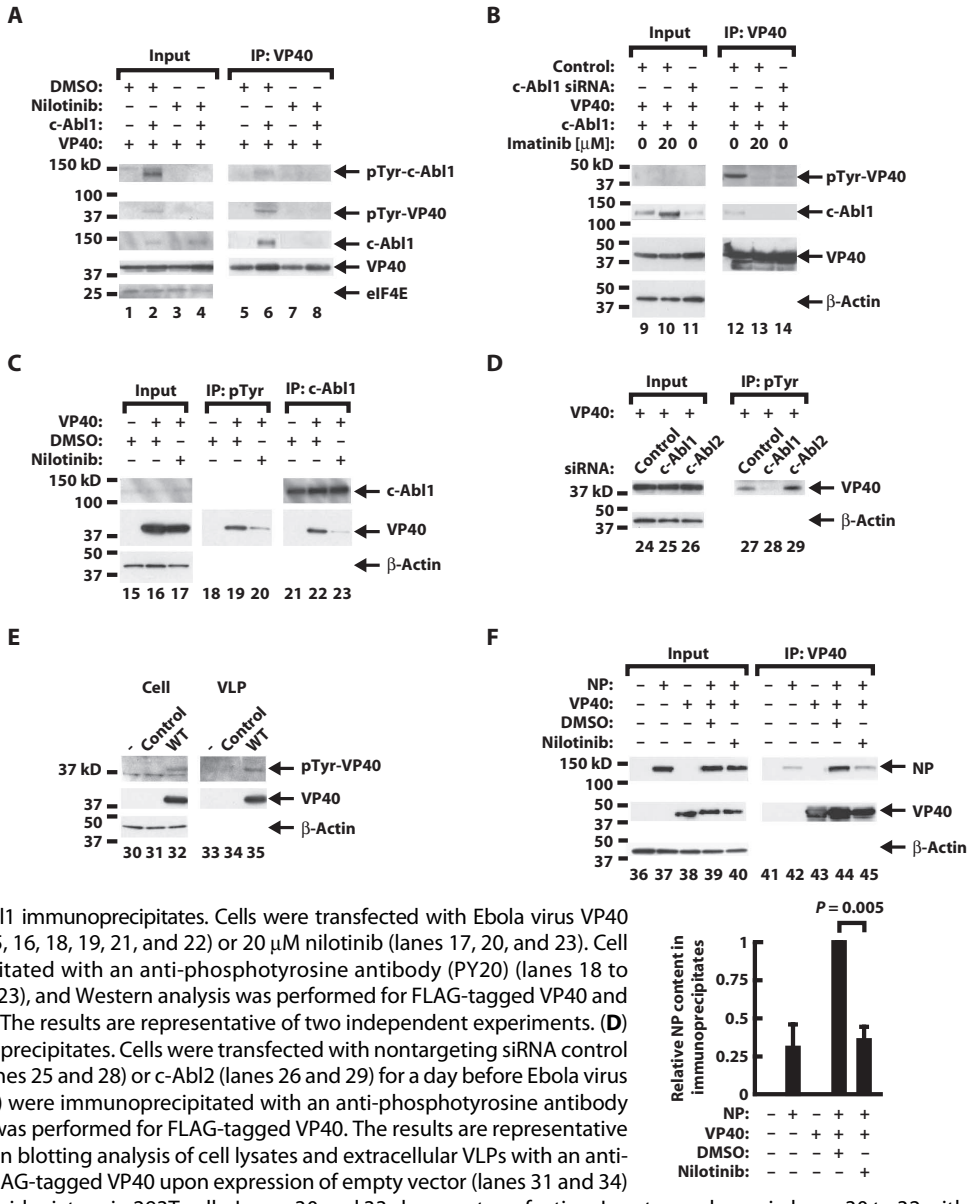

Fig. 4. Effect of c-Abl1 expression on VP40 phosphorylation and sensitivity to TK antagonist inhibition and siRNA. (**A**) Western analysis of transfected cell lysates (lanes 1 to 4) or VP40 immunoprecipitates (IP) (lanes 5 to 8) of cells transfected with empty vector control (lanes 1, 3, 5, and 7) or wild-type (WT) c-Abl1 (lanes 2, 4, 6, and 8) in the presence of VP40 expression vector. DMSO control (lanes 1 and 2 and lanes 5 and 6) or 20 μM nilotinib (lanes 3 and 4 and lanes 7 and 8) was added 12 to 18 hours after transfection. Kinase activity on VP40 was measured by Western analysis of inputs using an anti-phosphotyrosine (pTyr) antibody (upper panel). Western analysis was also performed for c-Abl1 and FLAG-tagged VP40 (middle panels). eIF4E was used as a loading control (lower panel). Analyses are representative of three independent experiments. (**B**) Western analysis of input cellular lysates (lanes 9 to 11) or VP40 immunoprecipitates (lanes 12 to 14) in cells transfected with nontargeting siRNA control (lanes 9, 10, 12, and 13) or a smart pool of siRNA targeting c-Abl1 (lanes 11 and 14) in the absence (lanes 9, 11, 12, and 14) or presence (lanes 10 and 13) of 20 μM imatinib. Kinase activity on VP40 was measured by Western analysis of inputs using an anti-phosphotyrosine antibody (upper panel). Western analysis was also performed for c-Abl1 and FLAG-tagged VP40 (middle panels). β-Actin was used as a loading control (lower panel). Analyses are representative of three independent experiments. (**C**) Western analysis of phosphotyrosine and c-Abl1 immunoprecipitates. Cells were transfected with Ebola virus VP40 and then treated with DMSO vehicle (lanes 15, 16, 18, 19, 21, and 22) or 20 μM nilotinib (lanes 17, 20, and 23). Cell lysates (lanes 15 to 17) were immunoprecipitated with an anti-phosphotyrosine antibody (PY20) (lanes 18 to 20) or anti–c-Abl1 antibody (8E9) (lanes 21 to 23), and Western analysis was performed for FLAG-tagged VP40 and c-Abl1. β-Actin was used as a loading control. The results are representative of two independent experiments. (**D**) Western analysis of phosphotyrosine immunoprecipitates. Cells were transfected with nontargeting siRNA control (lanes 24 and 27) or siRNA targeting c-Abl1 (lanes 25 and 28) or c-Abl2 (lanes 26 and 29) for a day before Ebola virus VP40 transfection. Cell lysates (lanes 24 to 26) were immunoprecipitated with an anti-phosphotyrosine antibody (PY20) (lanes 27 to 29), and Western analysis was performed for FLAG-tagged VP40. The results are representative of three independent experiments. (**E**) Western blotting analysis of cell lysates and extracellular VLPs with an anti-phosphotyrosine antibody (PY20) and anti–FLAG-tagged VP40 upon expression of empty vector (lanes 31 and 34) or WT VP40 (lanes 32 and 35) in the five-plasmid mixture in 293T cells. Lanes 30 and 33 show no transfection. Inputs are shown in lanes 30 to 32 with β-actin as a loading control. VLPs were purified by sucrose density sedimentation gradients. The results are representative of two independent experiments. (**F**) Coimmunoprecipitation of NP and VP40. Cells were cotransfected with NP and VP40 and then treated with DMSO (lanes 39 and 44) or 20 μM nilotinib (lanes 40 and 45). NP and FLAG-tagged VP40 in cell lysates (lanes 36 to 40) and VP40 immunoprecipitates (lanes 41 to 45) were detected by Western analysis using rabbit anti-NP antiserum and anti-FLAG mAb. β-Actin was used as a loading control. NP levels in VLPs were normalized to NP levels in lysates and then expressed as a ratio of the DMSO control sample (lower panel). Data are presented as means ± SEM from four independent experiments, and significance was analyzed by paired Student's *t* test.

that could be useful to corroborate our conclusions, transfection efficiency and rates of growth were different between knockout and parental cell lines, making comparisons inconclusive, and these cell lines cannot be infected by Ebola virus.

TKs including c-Abl1 interact with targets via a multistep process that results in stable recruitment and autoactivation of the kinase, and phosphorylation of the target protein (*27*–*30*). Stable recruitment of TKs occurs via interactions with its SH2 and SH3 domains, which respectively bind phosphotyrosine and proline-rich regions on target molecules (*17*, *27*–*30*). In accordance with these mechanisms, we found that c-Abl1 phosphorylates Y^{13} of VP40 and regulates the egress of Ebola virus from infected cells. In addition to inhibiting the Bcr-Abl kinase in cells from patients with chronic myelogenous leukemia, imatinib and nilotinib target c-Abl1 itself and other TKs, including Abl2, c-KIT, and platelet-derived growth factor receptor, although with differing potencies (*31*, *32*). Although we cannot exclude the possibility that these antagonists could exert additional effects through these kinases, the c-Abl1–specific knockdown and demonstration of c-Abl1 phosphorylation of VP40 Y^{13} suggest that the major pharmacological effect is exerted through c-Abl1 antagonism.

VP40 also contains a proline-rich region at its N terminus, which together with Y^{13} may serve to recruit Abl1 and facilitate morphogenesis and budding of virions (*17*, *22*, *24*). The overlapping late domains PTAP and PPxY in the N terminus of VP40 have been implicated in virus egress of pseudotyped lentiviral vectors (*19*, *33*), but their role in filoviruses has not been demonstrated (*34*). Although Tsg101 and Nedd4 interact with Ebola virus VP40 in the absence of other viral proteins and Nedd4 has been implicated in Ebola virus budding (*23*, *35*), a role for tyrosine phosphorylation in the regulation of this process has not been previously recognized and represents an interaction between host and viral proteins susceptible to pharmacological intervention. Furthermore, our experiments show that Nedd4 and VP40 play different roles in Ebola virus egress. Phosphorylation is a common mechanism to regulate protein function and is used in the context of proline-rich regions (*36*). Filovirus structural proteins are subject to cellular kinase and phosphatase activity (*37*), although specific sites of phosphorylation in different Ebola virus gene products and their requirement for viral replication have not been reported previously. For example, phosphorylation of NP, VP30, or GP of Marburg virus and

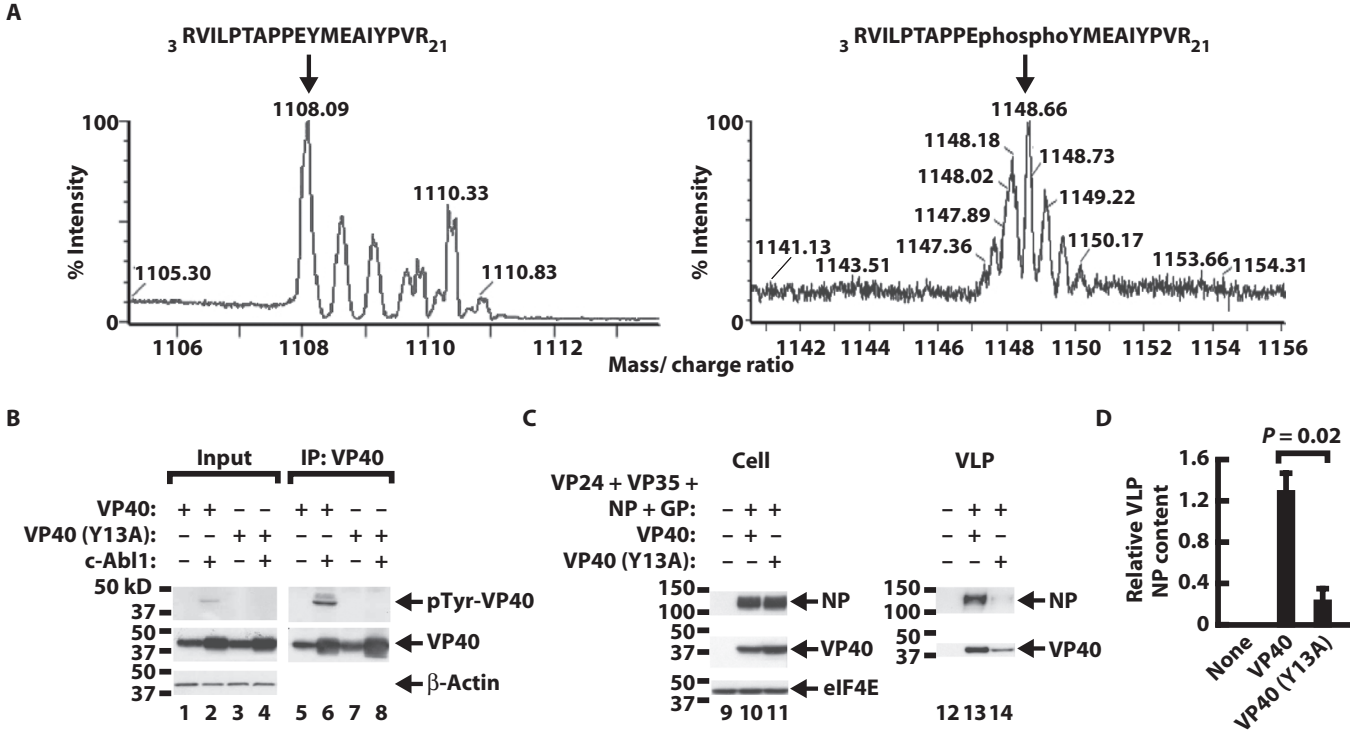

Fig. 5. Localization of VP40 c-Abl1–mediated tyrosine phosphorylation and effect of tyrosine mutation on VLP release. (**A**) Expanded region of the MALDI-TOF MS spectrum of the VP40 (amino acids 3 to 21) acquired for the nonphosphorylated (left) versus the phosphorylated (right) peptides from 293T cells cotransfected with VP40 and c-Abl1. Analysis was performed on a gel slice of a FLAG-tagged VP40 immunoprecipitate. Arrow indicates site of Y^{13} phosphorylation of VP40. (**B**) Western analysis of VP40 phosphorylation using WT or VP40 mutants created by site-directed mutagenesis on Y^{13}. Cells were transfected with empty vector control (lanes 1, 3, 5, and 7) or WT c-Abl1 vector (lanes 2, 4, 6, and 8) in the absence (lanes 1, 2, 5, and 6) or presence (lanes 3, 4, 7, and 8) of Y13A VP40 labeled with a FLAG tag. WT VP40 was used as a reference in both cases. Phosphorylation on tyrosine was measured by Western analysis (upper panel) in cell lysates (lanes 1 to 4) or in VP40 immunoprecipitates (lanes 5 to 8). Western analysis was also carried out for VP40 by FLAG labeling (middle panel). β-Actin was used as a loading control (lower panel). The results are representative of four independent experiments. (**C**) Western analysis of cell lysates and extracellular VLPs upon expression of empty vector (lanes 9 and 12), WT VP40 (lanes 10 and 13), or Y13A VP40 (lanes 11 and 14) Ebola virus VP40 in the five-plasmid mixture in 293T cells. Inputs are shown in lanes 9 to 11 with eIF4E as a loading control. VLPs were purified by sucrose density sedimentation gradients. The results are representative of three independent experiments. (**D**) Quantitation of the ratio of NP in VLPs relative to cell lysate NP based on (C) (lanes 9 to 11 and 12 to 14). Data are presented as means ± SEM of individual measures with cells from three independent experiments, and significance was analyzed using paired Student's *t* test.

Ebola virus has been suggested (*37*–*42*), but modification of specific amino acid residues on these proteins has not been described, and their role in viral replication has not been shown. Recent reports also indicate that Ebola virus VP35 can be phosphorylated in vitro by IKK-ε (inhibitor of nuclear factor κB kinase ε) and TBK-1 (TANK-binding kinase 1) (*43*), but the role these kinases play in regulating viral replication has not been established.

Several potential phosphorylation sites are present in VP40. VP40 has five tyrosine residues that could be the target of TKs such as c-Abl. Han and Harty also reported putative extracellular signal–regulated kinase (ERK) phosphorylation sites within the Ebola virus VP40 protein and suggested that ERK1/2 promote budding (*44*), but the specific modifications were not defined. Here, we show that Y^{13} in the PPxY motif, which is highly conserved in diverse Ebola virus strains, is a target of c-Abl1 modification and regulates Ebola virus egress. Although previous studies showed that this motif can substitute for a similar sequence in lentiviruses and support lentiviral particle formation (*34*), the present study demonstrates its role in Ebola virus egress, which differs substantially from lentiviral budding.

Previous work has established that certain bacteria and DNA viruses utilize Abl- or Src-family TKs during infection. For example, they may affect the release of orthopoxviruses (*7*, *9*) and the entry of polyomaviruses (*8*), as well as the pathogenesis of enteropathogenic *E. coli* (*6*) and *Shigella flexneri* (*5*, *6*). It is important to recognize, however, that the specific molecular targets that affect these pathogens differ from Ebola virus. During Ebola virus assembly, coexpression of NP and virion-associated proteins VP35 and VP24 leads to spontaneous formation of nucleocapsid-like structures in transfected 293T cells that are morphologically indistinguishable from nucleocapsids in virus-infected cells (*1*–*3*). Whereas VP40 appears critical for transport of nucleocapsids to the cell surface and for their incorporation into VLPs or virions, GP is not required (*2*). Therefore, an interaction between NP and VP40 is likely essential for these processes. In nucleocapsid assembly assays, nilotinib had no effect on the levels of NP and VP35, a result that suggests that nucleocapsid assembly is not dependent on c-Abl1. However, NP and VP40 levels are lower in VLPs with nilotinib treatment. Similar reductions in VP40 and NP levels were obtained with imatinib or with siRNAs specific to c-Abl1. Accordingly, we also observed a reduction in VLPs formed by VP40 alone in response to nilotinib or Abl-specific siRNAs. Finally, our data suggest that phosphorylation of VP40 may facilitate its association with NP because nilotinib abrogated this interaction. Together, these data suggest that nucleocapsid formation is not dependent on c-Abl1, but that c-Abl1 regulates either transport of nucleocapsid to the membrane and/or virion release, both of which depend on VP40. A delayed effect of the drug in infection of Vero cells and lack of effect of nilotinib in a pseudovirus infection assay also implicate c-Abl1 in late stages. Rather than modifying a cellular protein such as actin, whose assembly modulates viral or bacterial transport (*6*, *7*, *9*, *17*, *45*, *46*), c-Abl1 modulates the VP40 viral protein that modulates virion egress during infection, identifying this kinase as a target for an antiviral therapy.

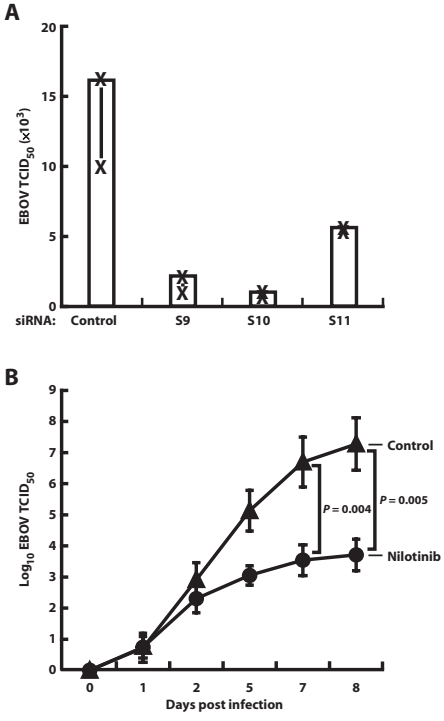

Fig. 6. Effect of siRNA knockdown and c-Abl1 TK inhibition on Ebola virus replication. (**A**) Effect of a nontargeted siRNA control or individual siRNAs targeting c-Abl1 (S9, S10, and S11) on Zaire strain Ebola virus (EBOV) release from Vero cells on day 7 after infection. Cells were infected at a multiplicity of infection (MOI) of 1. Background viral load for day 1 was subtracted. Data are presented as means ± SEM of individual measures with cells from two independent experiments. (**B**) Viral load was measured in supernatant fluids of Vero cells infected with Zaire strain Ebola virus and treated with nilotinib (20 μM). Viral load was measured by $TCID_{50}$ on days 0, 1, 2, 7, and 8 after infection compared to DMSO vehicle control. Background viral load for day 0 was subtracted. Data are presented as means ± SEM of four individual measures, and significance was analyzed by paired Student's *t* test.

Currently, there are no drugs available for use in prophylaxis or treatment of Ebola virus infection. Drugs that target filovirus budding would be expected to reduce the spread of infection, giving the immune system time to control the infection. In addition, budding inhibitors remain attractive therapeutics because they have the potential for broad-spectrum activity by interfering with a common pathway used by different viruses (*47*). As reported for the small molecules FGI-104 and FGI-106 (*47*–*49*), the Abl-family kinase inhibitors imatinib and nilotinib may be useful in this respect. Imatinib, marketed as Gleevec, is used to treat chronic myelogenous leukemia in humans (*50*), a disease caused by dysregulation of c-Abl (*10*, *15*), and nilotinib, also known as Tasigna, has been used in chronic myelogenous leukemia patients who exhibit resistance to Gleevec (*12*, *50*). Both compounds have reasonable safety profiles, although some cardiac toxicity has been reported with long-term administration in a small number of patients (*51*–*53*). Moreover, imatinib does not interfere with acquisition of protective immunity (*7*, *9*). Our results suggest that short-term administration of nilotinib or imatinib may be useful in treating Ebola virus infections. In this regard, targeting such invariant host gene products rather than the virus itself may reduce the likelihood that the virus will develop escape mutations and become drug-resistant.

MATERIALS AND METHODS

Cells

Human embryonic kidney (HEK) 293T, 293A cells, and Vero E6 cells were obtained from the American Type Culture Collection. Cells were

cultured in Dulbecco's modified Eagle's medium (DMEM) (Invitrogen) supplemented with 10% fetal bovine serum (FBS) and penicillin (100 U/ml) and streptomycin (100 μg/ml).

Virus

Ebola Zaire was provided by P. Jahrling. Human adenovirus 5 was obtained from the American Type Culture Collection.

Drugs

Imatinib mesylate and nilotinib were synthesized by W. Bornmann at M. D. Anderson Cancer Center.

Plasmids

Expression vectors pGP(Z), pNP, pVP24, pVP35, and pFLAG_VP40 contain a cytomegalovirus enhancer and promoter as described (*1*, *3*). pΔ8.2 and luciferase (*54*) were used in a pseudovirus infection assay in combination with pGP(Z) envelope. VP40 mutants were created by site-directed mutagenesis (Stratagene). c-Abl1 wild-type and kinase-dead plasmids (*55*) were provided by Y. Shaul (Weizmann Institute of Science, Israel). Nedd4 wild-type plasmid was obtained from Addgene.

Transient transfections

For the egress assay and electron microscopy, 2.5×10^5 HEK 293T cells were seeded in six-well plates. On the following day, the cells were transfected with 0.5 μg of pNP, pVP24, pVP35, wild-type, or mutant pFLAG_VP40 and 0.00625 μg of pGP(Z) with Lipofectamine 2000 (Invitrogen). The backbone plasmid was used as a negative control. For VP40 VLPs, the cells were transfected only with 0.5 μg of pFLAG_VP40. For phosphorylation studies, 0.5 μg of wild-type FLAG_VP40 or FLAG_VP40 mutants was transfected alone or in combination with 2 μg of wild-type c-Abl1 except for the experiment in which 0.5 μg of pFLAG_VP40 was cotransfected with 1 μg of wild-type c-Abl1 or kinase-dead c-Abl1 or when 1 μg of c-Abl1 was transfected alone. For siRNA experiments in the presence of VP40 and c-Abl1, 0.5 μg of FLAG_VP40 was transfected in combination with 1 μg of wild-type c-Abl1. For the interaction of VP40 and NP or Nedd4, cells were cotransfected with 1 μg of each plasmid. For the interaction of VP40 with c-Abl1, 0.5 μg of wild-type FLAG_VP40 or FLAG_VP40 mutants was transfected alone or in combination with 2 μg of wild-type c-Abl1. For nucleocapsid formation, the cells were cotransfected with 0.5 μg of pNP, pVP24, and pVP35. For endogenous c-Abl1 association or phosphorylation of VP40, 2.5×10^6 HEK 293T cells seeded in 10-cm plates were transfected with 5 μg of pFLAG_VP40. For cushion analysis of particle formation, 2.5×10^6 HEK 293T cells were transfected with 2 μg of pNP, pVP24, pVP35, wild-type, or mutant pFLAG_VP40 and 0.025 μg of pGP(Z). For electrospray ionization liquid chromatography–tandem MS (ESI-LC-MS/MS) studies, 2.5×10^6 HEK 293T cells were transfected with 5 μg of pFLAG_VP40 and 5 μg of c-Abl1 or plasmid control. When used, drugs were added 12 to 18 hours after transfection. Cells were harvested 36 to 48 hours later. Supernatant fluids were kept at 4°C, and cell pellets were frozen at −80°C.

Small interfering RNA

For siRNA experiments, 1.25×10^5 293T or Vero E6 cells per well were transfected with a total of 100 pmol of smart pools of siRNA for c-Abl1 (ON-TARGETplus SMARTpool L-003100-00-0005, Human ABL1, NM_005157) or c-Abl2 (ON-TARGETplus SMARTpool L-003101-00-0005, Human ABL2, NM_005158) (Dharmacon) with Lipofectamine 2000 (Invitrogen). Alternatively, three individual siRNAs against c-Abl1 (ON-TARGETplus J-003100-09-S9, J-003100-10-S10, and J-003100-11-S11, Human ABL1, NM_007313; NM_005157) (Dharmacon) were used at the same concentration. The following day, 293T cells were transfected for a second time with pGP(Z), pNP, pVP24, pVP35, and pFLAG_VP40 or pFLAG_VP40 alone. When siRNAs were used to study endogenous phosphorylation, 1.25×10^6 293T cells were transfected 1 day before VP40 at a concentration of 600 pmol in a 10-cm dish. Thirty-six to 48 hours later, cells were harvested. For Vero E6 cells, the transfection mixture was removed and the cells were infected at a multiplicity of infection (MOI) of 1 with Zaire Ebola virus for 2 hours. The inoculum was then removed, fresh medium was added, and supernatant fluids were collected on day 7 after infection. A nontargeting control siRNA was used as a reference.

Production of pseudotyped lentiviral viruses

The pseudotyped lentiviral vectors were produced by cotransfecting 293T cells with expression vectors pΔ8.2, luciferase, and pGP(Z) by Ca as previously reported (*54*). After 24 hours, the transfection mixture was removed and fresh medium was added. Seventy-two hours later, supernatant fluid was collected and filtered.

293A infection

Pseudotyped lentiviruses (100 μl) were added to cells that had been preincubated for 2 hours with 20 μM nilotinib or dimethyl sulfoxide (DMSO) in a final volume of 200 μl per well. Luciferase activity was measured after 48 hours as previously described (*56*) with mammalian cell lysis buffer and luciferase assay reagent (Promega).

Cell lysis and immunoprecipitation

Cell extracts for Western analysis and immunoprecipitations were resuspended in 450 ml of cell lysis buffer (Cell Signaling Technology) supplemented with a cocktail of protease (Roche) and phosphatase inhibitors (Sigma) for 30 min. Cells were pelleted for 5 min at 13,200 rpm. Aliquots (30 μl) of the soluble fraction were kept as loading control, and the remaining lysate was immunoprecipitated overnight at 4°C. For coimmunoprecipitation of VP40 and NP or Nedd4 or c-Abl1, the lysate was subjected to immunoprecipitation with anti-FLAG–coated beads (Sigma). For phosphorylation assays, lysates were immunoprecipitated with the same beads or with anti-phosphotyrosine (PY20) (Santa Cruz Biotechnology Inc.) or anti–c-Abl1 (8E9) (BD Biosciences) followed by protein G beads (Invitrogen) for an additional 3 hours at 4°C the next morning. For nucleocapsid formation, lysates were immunoprecipitated with polyclonal antibody anti-NP followed by protein G beads. Supernatant fluids were immunoprecipitated overnight at 4°C with a polyclonal antibody anti–Ebola virus GP obtained from immunized rabbits followed by protein G beads. For VP40 VLPs, supernatant fluids were immunoprecipitated overnight at 4°C with mAb anti-FLAG. For ESI-LC-MS/MS, cells were lysed and immunoprecipitated with protein G beads for 2 hours at 4°C for preclearance. After centrifugation, soluble lysates were incubated with beads covered with mAb anti-FLAG for an additional 3 hours at 4°C. In all the above cases, beads were pelleted, washed three times with cold 1× phosphate-buffered saline (Gibco), and resuspended in 30 μl of 1× loading buffer (Invitrogen). After 5 min of boiling, samples were loaded onto 4 to 15% polyacrylamide Criterion precast gels (Bio-Rad) under denaturing conditions. For MS/MS, bands corresponding to VP40 were excised after silver staining and sent for analysis.

Sucrose gradient sedimentation

Culture supernatants were clarified with low-speed centrifugation and a 0.45-μm filter and layered onto a 20% sucrose cushion. VLPs were pelleted through the cushion at 100,000*g* for 3 hours. Viral proteins in cell lysates and VLPs were analyzed by Western blotting.

Immunoblot assays

Protein lysates were transferred to polyvinylidene fluoride membranes and blocked for 1 hour at room temperature in 1× tris-buffered saline (TBS) + 0.1% Tween 20 + 2.5% (w/v) nonfat dry milk. Blots were incubated with primary antibodies at appropriate dilutions in the above buffer for an hour at room temperature or in 1× TBS + 0.1% Tween 20 + 5% (w/v) bovine serum albumin with gentle agitation overnight at 4°C according to the manufacturer's suggestion. Membranes were probed with 1:1000 dilution of primary antibodies against c-Abl1 (Bethyl), 1:1000 antibody against phospho–c-Abl (Y^{412}) or anti-Nedd4 (Cell Signaling Technology), c-Abl2 (2.5 μg/ml) (Abcam), 1:5000 antibody against Ebola virus–NP or Ebola virus–GP from DNA-immunized mice or rabbits, 1:3000 antibody against Ebola virus–VP35 from DNA-immunized guinea pigs, 1:100 of anti-phosphotyrosine (PY20) (Santa Cruz Biotechnology) or 4G10 (Millipore), VP40 (0.1 ng/μl) (IBT Bioservices), or 1:10,000 of anti-FLAG and 1:5000 of β-actin (Sigma), or 1:1000 of anti-eIF4E (Cell Signaling Technology) as loading controls. Secondary antibodies were alkaline phosphatase–conjugated anti-mouse or anti-rabbit immunoglobulin G (IgG) (Santa Cruz Biotechnology) or anti–guinea pig IgG (Jackson ImmunoResearch Laboratories Inc.). Secondary antibodies at a dilution of 1:5000 were added to 10 ml of 1× TBS + 0.1% Tween 20 + 2.5% (w/v) nonfat dry milk with gentle agitation for 1 hour at room temperature. Blots were washed and developed with ECL detection reagent (GE Healthcare). Semiquantitative analysis was performed with ImageQuant TL 7.0 image analysis software (GE Healthcare).

Infectivity assay

Vero cells cultured in DMEM (Invitrogen) containing D-glucose (4500 mg/liter) and L-glutamine and supplemented with 2% heat-inactivated FBS (DMEM-2) were incubated for 2 hours with 20 μM nilotinib before infection with Ebola Zaire for an additional 2 hours at an MOI of 1. The inoculum was then removed and fresh medium with the drug at the same concentration was added. DMSO vehicle was used as a negative control. Aliquots of supernatant fluids were taken at days 0, 1, 2, 5, 7, or 8 after infection for $TCID_{50}$ determination. For adenovirus 5 infection, we used the Adeno-X rapid titer kit and followed the protocol according to the manufacturer's indications (Clontech).

$TCID_{50}$ assay

The quantity of Ebola virus in samples was estimated by calculating the $TCID_{50}$ as described by Reed and Muench (*57*).

Electron microscopy

Forty-eight hours after transfection, 293T cells were harvested, fixed, and analyzed in the electron microscopy facility at the National Cancer Institute–Frederick.

Electrospray ionization liquid chromatography–tandem MS

Silver-stained gel bands were destained according to Gharahdaghi *et al.* (*58*). Gels were then reduced and alkylated. Digestion was carried out by adding 0.10 μg of modified trypsin (sequencing grade, Roche Molecular Biochemicals) in 50 μl of 0.025 M tris (pH 8.5). Peptides were extracted with 2× 50 μl of 50% acetonitrile + 2% trifluoroacetic acid, and the combined extracts were reduced in volume in a SpeedVac and brought up to 20 μl with 0.1% formic acid. Aliquots (5 μl) were analyzed by LC-MS/MS and performed on a Waters Ultima Q-TOF hybrid quadrupole/time-of-flight (TOF) mass spectrometer with a nanoelectrospray source. Chromatography was performed on an LC Packings HPLC (high-performance liquid chromatography) with a C18 PepMap column using a 2-hour linear acetonitrile gradient with a flow rate of 200 nl/min. Raw data files were processed with the MassLynx ProteinLynx software, and .pkl files were submitted for searching at http://www.matrixscience.com with the Mascot algorithm.

Cell viability and cytopathic effect

Vero cells were harvested 1, 2, 3, and 7 days and 293T cells 36 to 48 hours after the addition of 20 μM nilotinib or DMSO control. Cell viability was determined by exclusion of 7-aminoactinomycin D (7-AAD), a fluorescent chemical compound with a strong affinity for DNA, in a BD LSR cell analyzer (BD Biosciences) with FlowJo version 9.1 (TriStar Inc.). Cytopathic effect was estimated by visual examination of Vero E6 cell monolayers infected with Ebola virus several days after infection.

Statistical analysis

Data are expressed as means ± SEM. Paired Student's *t* test was used either between control and test drugs or test siRNAs, or wild-type versus mutant proteins. For statistical analysis, GraphPad Prism software was used. For all tests, a value of $P < 0.05$ was accepted as statistically significant.

SUPPLEMENTARY MATERIALS

www.sciencetranslationalmedicine.org/cgi/content/full/4/123/123ra24/DC1

Fig. S1. Transient transfection of NP, VP40, VP35, VP24, and GP gives rise to Ebola VLPs in 293T cells.
Fig. S2. GP levels in 293T cell lysates after drug treatment.
Fig. S3. Tyrosine phosphorylation of c-Abl1 and VP40 after expression of c-Abl1 in 293T cells.
Fig. S4. Analysis of VP40 modification in transfected 293T cells.
Fig. S5. Nedd4 and c-Abl1 interaction with VP40.
Fig. S6. Infection assays.

REFERENCES AND NOTES

1. Y. Huang, L. Xu, Y. Sun, G. J. Nabel, The assembly of Ebola virus nucleocapsid requires virion-associated proteins 35 and 24 and posttranslational modification of nucleoprotein. *Mol. Cell* **10**, 307–316 (2002).
2. T. Noda, H. Ebihara, Y. Muramoto, K. Fujii, A. Takada, H. Sagara, J. H. Kim, H. Kida, H. Feldmann, Y. Kawaoka, Assembly and budding of Ebolavirus. *PLoS Pathog.* **2**, e99 (2006).
3. W. Shi, Y. Huang, M. Sutton-Smith, B. Tissot, M. Panico, H. R. Morris, A. Dell, S. M. Haslam, J. Boyington, B. S. Graham, Z. Y. Yang, G. J. Nabel, A filovirus-unique region of Ebola virus nucleoprotein confers aberrant migration and mediates its incorporation into virions. *J. Virol.* **82**, 6190–6199 (2008).
4. G. Ruthel, G. L. Demmin, G. Kallstrom, M. P. Javid, S. S. Badie, A. B. Will, T. Nelle, R. Schokman, T. L. Nguyen, J. H. Carra, S. Bavari, M. J. Aman, Association of Ebola virus matrix protein VP40 with microtubules. *J. Virol.* **79**, 4709–4719 (2005).
5. E. A. Burton, R. Plattner, A. M. Pendergast, Abl tyrosine kinases are required for infection by *Shigella flexneri*. *EMBO J.* **22**, 5471–5479 (2003).
6. A. Swimm, B. Bommarius, Y. Li, D. Cheng, P. Reeves, M. Sherman, D. Veach, W. Bornmann, D. Kalman, Enteropathogenic *Escherichia coli* use redundant tyrosine kinases to form actin pedestals. *Mol. Biol. Cell* **15**, 3520–3529 (2004).
7. P. M. Reeves, B. Bommarius, S. Lebeis, S. McNulty, J. Christensen, A. Swimm, A. Chahroudi, R. Chavan, M. B. Feinberg, D. Veach, W. Bornmann, M. Sherman, D. Kalman, Disabling poxvirus pathogenesis by inhibition of Abl-family tyrosine kinases. *Nat. Med.* **11**, 731–739 (2005).
8. A. I. Swimm, W. Bornmann, M. Jiang, M. J. Imperiale, A. E. Lukacher, D. Kalman, Abl family tyrosine kinases regulate sialylated ganglioside receptors for polyomavirus. *J. Virol.* **84**, 4243–4251 (2010).
9. P. M. Reeves, S. K. Smith, V. A. Olson, S. H. Thorne, W. Bornmann, I. K. Damon, D. Kalman, Variola and monkeypox viruses utilize conserved mechanisms of virion motility and release that depend on Abl and Src family tyrosine kinases. *J. Virol.* **85**, 21–31 (2011).

10. C. L. Sawyers, Chronic myeloid leukemia. *N. Engl. J. Med.* **340**, 1330–1340 (1999).
11. J. M. Goldman, B. J. Druker, Chronic myeloid leukemia: Current treatment options. *Blood* **98**, 2039–2042 (2001).
12. M. Golemovic, S. Verstovsek, F. Giles, J. Cortes, T. Manshouri, P. W. Manley, J. Mestan, M. Dugan, L. Alland, J. D. Griffin, R. B. Arlinghaus, T. Sun, H. Kantarjian, M. Beran, AMN107, a novel aminopyrimidine inhibitor of Bcr-Abl, has in vitro activity against imatinib-resistant chronic myeloid leukemia. *Clin. Cancer Res.* **11**, 4941–4947 (2005).
13. T. O'Hare, D. K. Walters, M. W. Deininger, B. J. Druker, AMN107: Tightening the grip of imatinib. *Cancer Cell* **7**, 117–119 (2005).
14. E. Weisberg, P. Manley, J. Mestan, S. Cowan-Jacob, A. Ray, J. D. Griffin, AMN107 (nilotinib): A novel and selective inhibitor of *BCR-ABL*. *Br. J. Cancer* **94**, 1765–1769 (2006).
15. B. J. Druker, Translation of the Philadelphia chromosome into therapy for CML. *Blood* **112**, 4808–4817 (2008).
16. J. M. Licata, R. F. Johnson, Z. Han, R. N. Harty, Contribution of Ebola virus glycoprotein, nucleoprotein, and VP24 to budding of VP40 virus-like particles. *J. Virol.* **78**, 7344–7351 (2004).
17. B. Bommarius, D. Maxwell, A. Swimm, S. Leung, A. Corbett, W. Bornmann, D. Kalman, Enteropathogenic *Escherichia coli* Tir is an SH2/3 ligand that recruits and activates tyrosine kinases required for pedestal formation. *Mol. Microbiol.* **63**, 1748–1768 (2007).
18. B. Hartlieb, W. Weissenhorn, Filovirus assembly and budding. *Virology* **344**, 64–70 (2006).
19. R. N. Harty, M. E. Brown, G. Wang, J. Huibregtse, F. P. Hayes, A PPxY motif within the VP40 protein of Ebola virus interacts physically and functionally with a ubiquitin ligase: Implications for filovirus budding. *Proc. Natl. Acad. Sci. U.S.A.* **97**, 13871–13876 (2000).
20. L. D. Jasenosky, Y. Kawaoka, Filovirus budding. *Virus Res.* **106**, 181–188 (2004).
21. C. A. Zampieri, N. J. Sullivan, G. J. Nabel, Immunopathology of highly virulent pathogens: Insights from Ebola virus. *Nat. Immunol.* **8**, 1159–1164 (2007).
22. T. Noda, H. Sagara, E. Suzuki, A. Takada, H. Kida, Y. Kawaoka, Ebola virus VP40 drives the formation of virus-like filamentous particles along with GP. *J. Virol.* **76**, 4855–4865 (2002).
23. J. Timmins, G. Schoehn, S. Ricard-Blum, S. Scianimanico, T. Vernet, R. W. Ruigrok, W. Weissenhorn, Ebola virus matrix protein VP40 interaction with human cellular factors Tsg101 and Nedd4. *J. Mol. Biol.* **326**, 493–502 (2003).
24. T. Hoenen, N. Biedenkopf, F. Zielecki, S. Jung, A. Groseth, H. Feldmann, S. Becker, Oligomerization of Ebola virus VP40 is essential for particle morphogenesis and regulation of viral transcription. *J. Virol.* **84**, 7053–7063 (2010).
25. R. F. Johnson, P. Bell, R. N. Harty, Effect of Ebola virus proteins GP, NP and VP35 on VP40 VLP morphology. *Virol. J.* **3**, 31 (2006).
26. Y. Liu, L. Cocka, A. Okumura, Y. A. Zhang, J. O. Sunyer, R. N. Harty, Conserved motifs within Ebola and Marburg virus VP40 proteins are important for stability, localization, and subsequent budding of virus-like particles. *J. Virol.* **84**, 2294–2303 (2010).
27. J. M. Smith, B. J. Mayer, Abl: Mechanisms of regulation and activation. *Front. Biosci.* **7**, d31–d42 (2002).
28. J. E. Dueber, B. J. Yeh, K. Chak, W. A. Lim, Reprogramming control of an allosteric signaling switch through modular recombination. *Science* **301**, 1904–1908 (2003).
29. J. E. Dueber, B. J. Yeh, R. P. Bhattacharyya, W. A. Lim, Rewiring cell signaling: The logic and plasticity of eukaryotic protein circuitry. *Curr. Opin. Struct. Biol.* **14**, 690–699 (2004).
30. M. Karplus, J. Kuriyan, Molecular dynamics and protein function. *Proc. Natl. Acad. Sci. U.S.A.* **102**, 6679–6685 (2005).
31. A. Pardanani, A. Tefferi, Imatinib targets other than *bcr/abl* and their clinical relevance in myeloid disorders. *Blood* **104**, 1931–1939 (2004).
32. F. J. Giles, M. O'Dwyer, R. Swords, Class effects of tyrosine kinase inhibitors in the treatment of chronic myeloid leukemia. *Leukemia* **23**, 1698–1707 (2009).
33. G. Neumann, H. Ebihara, A. Takada, T. Noda, D. Kobasa, L. D. Jasenosky, S. Watanabe, J. H. Kim, H. Feldmann, Y. Kawaoka, Ebola virus VP40 late domains are not essential for viral replication in cell culture. *J. Virol.* **79**, 10300–10307 (2005).
34. J. Martin-Serrano, D. Perez-Caballero, P. D. Bieniasz, Context-dependent effects of L domains and ubiquitination on viral budding. *J. Virol.* **78**, 5554–5563 (2004).
35. J. Yasuda, M. Nakao, Y. Kawaoka, H. Shida, Nedd4 regulates egress of Ebola virus-like particles from host cells. *J. Virol.* **77**, 9987–9992 (2003).
36. S. L. Pelech, J. S. Sanghera, Mitogen-activated protein kinases: Versatile transducers for cell signaling. *Trends Biochem. Sci.* **17**, 233–238 (1992).
37. O. Dolnik, L. Kolesnikova, S. Becker, Filoviruses: Interactions with the host cell. *Cell. Mol. Life Sci.* **65**, 756–776 (2008).
38. L. H. Elliott, M. P. Kiley, J. B. McCormick, Descriptive analysis of Ebola virus proteins. *Virology* **147**, 169–176 (1985).
39. S. Becker, S. Huppertz, H. D. Klenk, H. Feldmann, The nucleoprotein of Marburg virus is phosphorylated. *J. Gen. Virol.* **75** (Pt. 4), 809–818 (1994).
40. J. Modrof, C. Möritz, L. Kolesnikova, T. Konakova, B. Hartlieb, A. Randolf, E. Mühlberger, S. Becker, Phosphorylation of Marburg virus VP30 at serines 40 and 42 is critical for its interaction with NP inclusions. *Virology* **287**, 171–182 (2001).
41. C. Sänger, E. Mühlberger, B. Lötfering, H. D. Klenk, S. Becker, The Marburg virus surface protein GP is phosphorylated at its ectodomain. *Virology* **295**, 20–29 (2002).
42. M. J. Martínez, N. Biedenkopf, V. Volchkova, B. Hartlieb, N. Alazard-Dany, O. Reynard, S. Becker, V. Volchkov, Role of Ebola virus VP30 in transcription reinitiation. *J. Virol.* **82**, 12569–12573 (2008).
43. K. C. Prins, W. B. Cárdenas, C. F. Basler, Ebola virus protein VP35 impairs the function of interferon regulatory factor-activating kinases IKKε and TBK-1. *J. Virol.* **83**, 3069–3077 (2009).
44. Z. Han, R. N. Harty, Influence of calcium/calmodulin on budding of Ebola VLPs: Implications for the involvement of the Ras/Raf/MEK/ERK pathway. *Virus Genes* **35**, 511–520 (2007).
45. N. Scaplehorn, A. Holmström, V. Moreau, F. Frischknecht, I. Reckmann, M. Way, Grb2 and Nck act cooperatively to promote actin-based motility of vaccinia virus. *Curr. Biol.* **12**, 740–745 (2002).
46. T. P. Newsome, I. Weisswange, F. Frischknecht, M. Way, Abl collaborates with Src family kinases to stimulate actin-based motility of vaccinia virus. *Cell. Microbiol.* **8**, 233–241 (2006).
47. M. J. Aman, M. S. Kinch, K. Warfield, T. Warren, A. Yunus, S. Enterlein, E. Stavale, P. Wang, S. Chang, Q. Tang, K. Porter, M. Goldblatt, S. Bavari, Development of a broad-spectrum antiviral with activity against Ebola virus. *Antiviral Res.* **83**, 245–251 (2009).
48. M. S. Kinch, A. S. Yunus, C. Lear, H. Mao, H. Chen, Z. Fesseha, G. Luo, E. A. Nelson, L. Li, Z. Huang, M. Murray, W. Y. Ellis, L. Hensley, J. Christopher-Hennings, G. G. Olinger, M. Goldblatt, FGI-104: A broad-spectrum small molecule inhibitor of viral infection. *Am. J. Transl. Res.* **1**, 87–98 (2009).
49. Y. Liu, R. N. Harty, Viral and host proteins that modulate filovirus budding. *Future Virol.* **5**, 481–491 (2010).
50. P. Ault, Overview of second-generation tyrosine kinase inhibitors for patients with imatinib-resistant chronic myelogenous leukemia. *Clin. J. Oncol. Nurs.* **11**, 125–129 (2007).
51. R. Kerkelä, L. Grazette, R. Yacobi, C. Iliescu, R. Patten, C. Beahm, B. Walters, S. Shevtsov, S. Pesant, F. J. Clubb, A. Rosenzweig, R. N. Salomon, R. A. Van Etten, J. Alroy, J. B. Durand, T. Force, Cardiotoxicity of the cancer therapeutic agent imatinib mesylate. *Nat. Med.* **12**, 908–916 (2006).
52. R. Salie, R. T. Silver, Uncommon or delayed adverse events associated with imatinib treatment for chronic myeloid leukemia. *Clin. Lymphoma Myeloma Leuk.* **10**, 331–335 (2010).
53. H. R. Mellor, A. R. Bell, J. P. Valentin, R. R. A. Roberts, Cardiotoxicity associated with targeting kinase pathways in cancer. *Toxicol. Sci.* **120**, 14–32 (2011).
54. W. P. Kong, C. Hood, Z. Y. Yang, C. J. Wei, L. Xu, A. Garciá-Sastre, T. M. Tumpey, G. J. Nabel, Protective immunity to lethal challenge of the 1918 pandemic influenza virus by vaccination. *Proc. Natl. Acad. Sci. U.S.A.* **103**, 15987–15991 (2006).
55. R. Agami, G. Blandino, M. Oren, Y. Shaul, Interaction of c-Abl and p73α and their collaboration to induce apoptosis. *Nature* **399**, 809–813 (1999).
56. Z. Y. Yang, Y. Huang, L. Ganesh, K. Leung, W. P. Kong, O. Schwartz, K. Subbarao, G. J. Nabel, pH-dependent entry of severe acute respiratory syndrome coronavirus is mediated by the spike glycoprotein and enhanced by dendritic cell transfer through DC-SIGN. *J. Virol.* **78**, 5642–5650 (2004).
57. L. J. Reed, H. Muench, A simple method of estimating fifty per cent endpoints. *Am. J. Hygiene* **27**, 493–497 (1938).
58. F. Gharahdaghi, C. R. Weinberg, D. A. Meagher, B. S. Imai, S. M. Mische, Mass spectrometric identification of proteins from silver-stained polyacrylamide gel: A method for the removal of silver ions to enhance sensitivity. *Electrophoresis* **20**, 601–605 (1999).

Acknowledgments: We thank M. A. Gawinowicz from the Protein Core Facility at Columbia University for MS analyses, Y. Shaul for c-Abl1 plasmids, B. Hartman and J. Farrar for figure preparation, A. Tislerics for manuscript editing, and members of the Nabel laboratory for discussions and advice. We also thank J. Nunneley from Texas Biomed for BSL4 technical assistance. **Funding:** This research was supported by the Intramural Research Program of the Vaccine Research Center, National Institute of Allergy and Infectious Diseases, U.S. NIH. Live Ebola virus assays were conducted in Texas Biomed facilities constructed with support from the Research Facilities Improvement Program (grant number C06 RR012087) from the National Center for Research Resources. **Author contributions:** M.G. designed and performed the experiments and analyzed the data. A.C. designed experiments and analyzed the data. R.C. contributed to design and execution of BSL4 experiments. W.S. prepared and provided plasmids along with technical advice. W.B. synthesized the drugs used in these studies. D.K. and G.J.N. designed the experiments, analyzed the data, and provided strategic guidance. M.G., D.K., and G.J.N. participated in writing the paper. **Competing interests:** M.G., A.C., D.K., and G.J.N. are listed on the following patent, "C-Abl Tyrosine Kinase Inhibitors Useful For Inhibiting Filovirus Replication" #61/447,298, filed by the NIH. D.K. is listed on additional intellectual property applications filed by Emory University related to tyrosine kinases, and is entitled to royalties from Inhibikase Pharmaceuticals. The terms of this arrangement have been reviewed and approved by Emory University in accordance with its conflict-of-interest policies. The other authors declare that they no competing interests.

Submitted 22 November 2011
Accepted 9 February 2012
Published 29 February 2012
10.1126/scitranslmed.3003500

Citation: M. García, A. Cooper, W. Shi, W. Bornmann, R. Carrion, D. Kalman, G. J. Nabel, Productive replication of Ebola virus is regulated by the c-Abl1 tyrosine kinase. *Sci. Transl. Med.* **4**, 123ra24 (2012).

Science Translational Medicine

Productive Replication of Ebola Virus Is Regulated by the c-Abl1 Tyrosine Kinase

Mayra García, Arik Cooper, Wei Shi, William Bornmann, Ricardo Carrion, Daniel Kalman and Gary J. Nabel

Sci Transl Med **4**, 123ra24123ra24.
DOI: 10.1126/scitranslmed.3003500

Disabling Ebola virus

Ebola virus causes severe, often fatal, hemorrhagic fever in humans and is well known for its fulminant replication that ultimately overwhelms the capacity of the human immune system to contain it. Because it is easily transmitted from one human to another and causes high mortality, Ebola virus has been classified as a category A agent, the highest-priority biological threat classification. There are no effective prophylactic or therapeutic interventions available to treat infections with Ebola virus or another highly pathogenic filovirus, Marburg virus. Information about mechanisms of assembly and release of these viruses will be crucial for developing effective countermeasures.

Viruses exploit a variety of components within the host cell to complete their life cycles. In a new study, García *et al.* show that the growth of Ebola virus is regulated by the c-Abl1 tyrosine kinase. They demonstrate that release of Ebola virus–like particles in a cell culture cotransfection system could be blocked by c-Abl1–specific small interfering RNAs (siRNAs) or by Abl-specific kinase inhibitors such as nilotinib. They show that this effect is mediated by tyrosine phosphorylation of the Ebola matrix protein VP40. The researchers identified at least one site of tyrosine phosphorylation (Y^{13}) on VP40 and demonstrated that mutation of this residue reduced release of Ebola virus–like particles. The drug nilotinib or siRNAs directed against c-Abl1 also reduced productive replication of the Zaire strain of Ebola virus in cultured Vero cells by up to four orders of magnitude. Together, these data indicate that the c-Abl1 tyrosine kinase regulates budding or release of Ebola virus through a mechanism involving phosphorylation of VP40. The authors propose that this critical interaction between a viral and a host cell protein represents a target for antiviral therapy. These findings suggest that drugs such as nilotinib that inhibit c-Abl1 and are already in clinical use as anticancer therapeutics may be useful for reducing the severity of Ebola virus infection.

Science Translational Medicine (ISSN 1946-6242) is published by the American Association for the Advancement of Science, 1200 New York Avenue NW, Washington, DC 20005. The title *Science Translational Medicine* is a registered trademark of AAAS.